TECHNICAL UNIVERSITY OF CLUJ-NAPOCA

ACTA TECHNICA NAPOCENSIS

Series: Applied Mathematics, Mechanics, and Engineering
Vol. 69, Issue Special I, February, 2026

MODELING AND SIMULATION OF VARIOUS ADVANCED MATERIALS PARAMETERS FOR ELECTROCHEMICAL MACHINING

Titi DANCIU, Liviu-Daniel GHICULESCU

Abstract: *This paper presents multiple numerical simulations of different parameters of advanced materials for the electrochemical machining (ECM) process using COMSOL Multiphysics software. Since it is not possible to physically observe and record the processes taking place in the workspace, process modeling is one of the most effective methods to estimate the conditions in the workspace. In this context, numerical simulation of the electrochemical process becomes essential for its understanding and optimization. The electrochemical machining process's electric potential and the impact of the electric field were analyzed on a variety of advanced materials in order to enhance the quality of the ECM process.*
Key words: *modeling, simulation, electric field, electric potential, electrolyte*

1. INTRODUCTION

Electrochemical machining technology has seen a resurgence in recent years due to the usage of more advanced materials in aircraft engines and the rise in demand for turbomachinery components [1]. Another reason is that as the aerospace, automotive, and medical industries rapidly advance in accuracy and downsizing, many mechanical parts now contain tiny holes with unique shapes and groove structures [2][3][4][5]. Since it is not possible to physically observe and record the processes taking place in the inter-electrod gap, process modeling is one of the most effective methods for estimating the conditions.

Temperature, electric field, flow field, and other fields are all involved in electrochemical machining (ECM). The distribution of electrical conductivity is completely impacted by temperature and bubbles. The conductivity will progressively drop as the electrolyte flowing in the machining gap brings warmth and hydrogen to the output and builds up there [6]. It is challenging to forecast the ECM process precisely since changes in one aspect would result in changes in other physical domains. This is because erosion causes the interface shape between the electrolyte and work piece to change constantly within the solution range. The absence of selective erosion control distinguishes the ECM process from other machining techniques. Additionally, this processing occurs continually at varying rates along the whole surface of the work item.

2. MODELING AND SIMULATING THE ELECTRIC FIELD AND ELECTRIC POTENTIAL

Numerous attempts have been made to acquire data regarding ECM processing using numerical computer methods for various work settings. Chen et al. [6] thoroughly examined a number of variables to develop a coupling model involving the electric flow, temperature, and structural field. By simulating the electrolyte flow rate and pressure distribution in various tubular electrodes of electrochemical machining, Yao et al. [7] were able to get improved hole machining outcomes free of disruptions and sparks. The impact of the inter-electrode gap flow field distribution on the stability and precision of the blade's cooling holes was examined by Chai et al. [8]. Liu et al. [9] investigated the surface quality of the titanium alloy following electrochemical jet

processing. Simulations and experiments show that high processing quality can be attained. Using the finite element method, Patro et al. [10] forecasted how the workpiece's anode shape would change during electrochemical machining. A multi-field coupling model was developed by Zhou et al. [11] to model the impact of low speed electrolyte and hydrogen bubbles close to the cathode on heat transfer during ECM. The impact of the pertinent microporous electrochemical machining parameters on the rate of material removal and overcutting was investigated by Chandrasekhar et al. [12] using the Entropy VIKOR method. Liu et al. [12] developed the electric field model of through-mask micro-electrochemical machining with a moving tool using FEM. The impacts of the parameters on the machining shape were examined, including the thickness of the mask and the applied voltage. The findings demonstrate that a higher applied voltage results in a greater machining depth and width as well as a better aspect ratio. A thin mask results in an unevenly distributed electric field and more severe lateral corrosion.

In order to reduce stray corrosion in trepanning ECM, Hu et al. [14] used forward-flowing compressed air to create a gas film on the machined surface by blowing into the cathode. According to their research, the gas film layer may eliminate stray corrosion and taper angle while also enhancing the workpiece's machining surface quality and precision.

In this context, numerical simulation of the ECM becomes essential for its understanding and optimization. COMSOL Multiphysics is one of the most widely used software solutions in this field, providing an integrated framework for coupled modeling of mass transport, electric charge transfer and fluid-dynamic interactions in the electrochemical cell etc [15]. The simulations performed in COMSOL allowed me to predict the electric field distribution and electric potential distribution. It is also possible to predict electrode wear, the formation of by-products or heat accumulation, all of which are difficult to observe directly during physical experiments.

By integrating numerical simulation with practical experimentation, electrochemical machining research becomes more efficient, reducing the costs and time required to develop new technologies and prototypes. This approach contributes to the maturation of ECM processes and their expansion into high-precision applications, where traditional methods are no longer effective or applicable.

2.1 Creation of the models

COMSOL Multiphysics is used in this article to simulate the electric field and electric potential. The simulation process involved three stages: pre-processing, solution, and post-processing [16]. In the pre-processing stage, I established and built the fundamentals of the models, including the geometric structure. Also, here I chose the materials used, their properties, the domain, the boundary conditions, and the mesh elements. Regardless of whether the study is stationary or time-dependent, in the solution stage, also known as the execution stage, I performed the simulation using a relevant mathematical model of differential equations. Finally, in the post-processing stage, I interpreted the obtained results where I was able to create graphs for different types of variables or parameters. For the simulated models, I chose a 3D graphical representation. A representation for the interconnection of the relationships between the simulation solution stages can be seen in Figure 1.

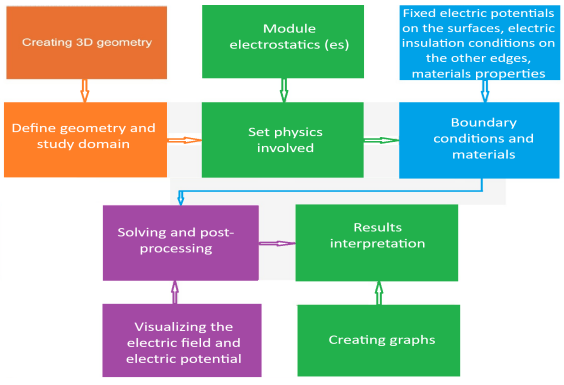

Fig. 1. The interconnection of the research stages

For my simulation in COMSOL, regarding the electric field and the electric potential, I created a new model, then I selected the modeling type, namely 3D modeling. After selecting in the AC/DC module, the “electrostatics”, I chose for my study the stationary type. Also, I configured the domain

geometry (workpiece, electrolyte, tool). Furthermore, I defined the materials and chose the physics for the study, namely electrostatics. For the anode, I applied an electric potential of 10 V (Model 1 and 2) and 15 V (Model 3). For the cathode, I applied an electric potential of -10 V (Model 1 and 2) and -15 V (Model 3). After creating the mesh elements, I chose the "extra-fine" option as the element size and selected the creation of all elements.

To complete the simulation, I selected the study and then its calculation. The visualization of the electric field and electric potential can be seen in the results section. Here we can also visualize the distribution of the electric field and electric potential.

By using the COMSOL Multiphysics software, I was able to solve the charge conservation equation for the electric potential, given the spatial distribution of the electric charge. Here, I was able to specify the working parameters such as: permittivity, polarization or permanent electric displacement of the material that I used in the constitutive relation.

2.2 Models conditions

For the simulation, I assumed that a constant value remains in the inter-electrod gap. The simulation of the electric field and electric potential were performed under different conditions. The simulation conditions used were the following:

1. **Model 1**- the cathode was made of 99% purity copper; the workpiece was made of a nickel-chromium alloy ($Ni_{61.4}Cr_{25.9}Mo_{11}Si_{1.5}$); for the electrolyte, I used a 10% concentration $NaNO_3$ solution and applied a voltage of 10 V.
2. **Model 2-** the cathode was made of 99% purity copper; the workpiece was made of a chromium-cobalt alloy Co-Cr ($Co_{60}Cr_{24.5}W_9Nb_{6.4}V_2Mo_{1.1}Si_{0.9}$); for the electrolyte, I used a 5% concentration NaCl solution and applied a voltage of 10 V.
3. **Model 3-** the cathode was made of 99% purity copper; The workpiece was constructed from a chromium-cobalt alloy Co-Cr ($Co_{60}Cr_{24.5}W_9Nb_{6.4}V_2Mo_{1.1}Si_{0.9}$), for the electrolyte I used a 5% NaCl solution and applied a voltage of 15 V.

The properties of the anode, cathode and electrolyte for Model 1 are shown in Table 1:

Table 1.

Material properties for Model 1 [17]

Property	Value	UM
Cathode relative permittivity (Cu, 99%)	1	1
Relative permittivity electrolyte ($NaNO_3$, 10%)	75	1
Anode relative permittivity ($Ni_{61.4}Cr_{25.9}Mo_{11}Si_{1.5}$)	2.5	1

In Figure 2 we can see the geometry of Model 1. The anode and cathode have dimensions L x w x h: 40x30x15 mm. The inter-electrod gap size is 0.7 mm.

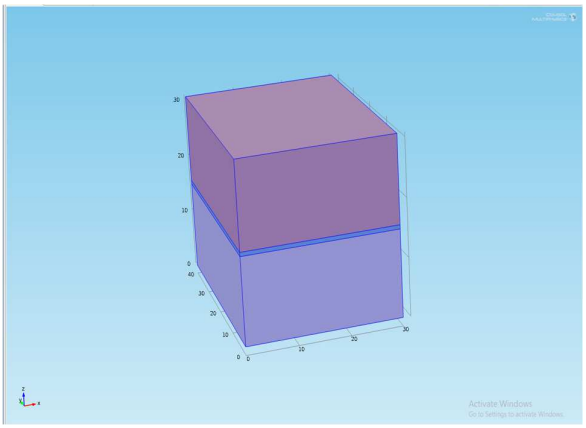

Fig. 2. Geometry for Model 1

In Figure 3 we have the representation of the mesh elements for Model 1. For this model I chose the extra-fine option as the element size.

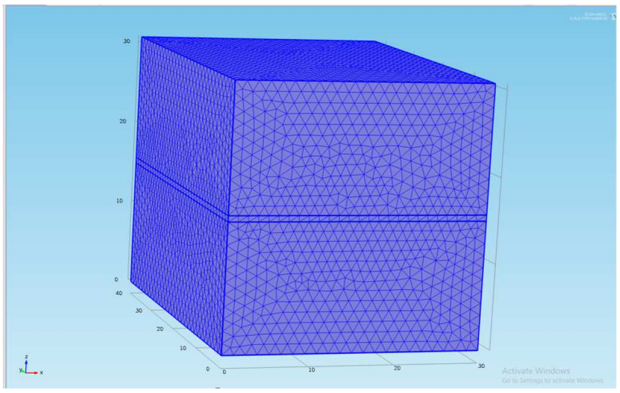

Fig. 3. The mesh elements for Model 1

In Figure 4 we have the representation of the electric potential for Model 1. It can be seen that

the distribution of the electric potential is uniform along the workpiece.

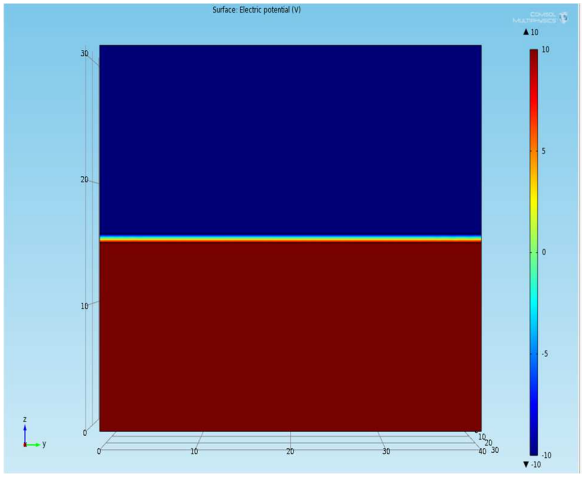

Fig. 4. Electric potential distribution for Model 1

Figure 5 illustrates the electric field distribution. The maximum intensity is recorded at the intersection between the anode and cathode. Also, the electric field distribution is uniform along the workpiece.

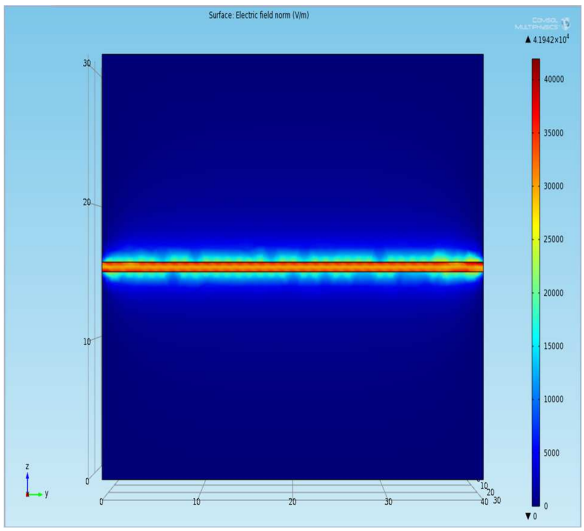

Fig. 5. Electric field distribution for Model 1

The properties of the anode, cathode and electrolyte for Model 2 are shown in Table 2:

Table 2.

Material properties for Model 2 [17]

Property	Value	UM
Cathode relative permittivity (Cu, 99%)	1	1
Relative permittivity electrolyte (NaCl, 5%)	72	1
Anode relative permittivity ($Co_{60}Cr_{24.5}W_9Nb_{6.4}V_2Mo_{1.1}Si_{0.9}$)	1	1

In the Model 2 and Model 3, the anode and cathode have the dimensions: r x h= 10 x 10 mm. The inter-electrod gap size is 0.8 mm.

Figure 6 shows the electrical potential for Model 2. The workpiece is connected to the positive terminal of the circuit (10 V), and the tool is connected to the negative terminal (-10 V).

Figure 7 shows the electric field distribution for Model 2. The maximum intensity is recorded at the intersection between the anode and cathode. Also, the electric field distribution is uniform along the workpiece.

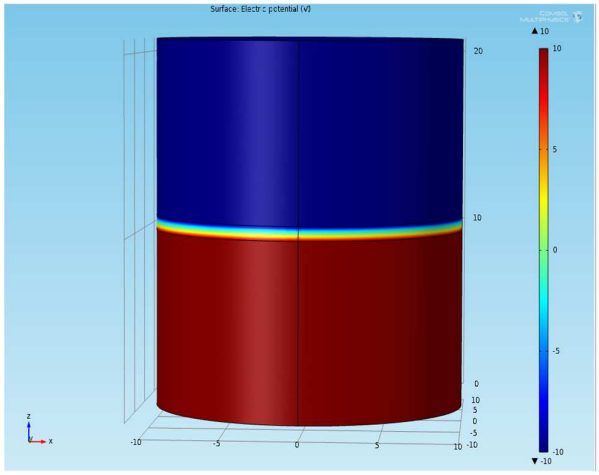

Fig. 6. Electric potential distribution Model 2

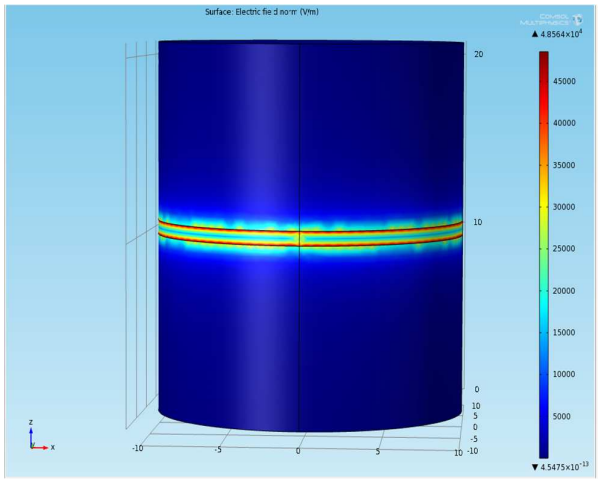

Fig. 7. Electric field distribution Model 2

Study 3 presents a simulation of Model 2, but with a change in the applied voltage. In Figure 8

we observe the electrical potential for Model 3. The workpiece is connected to the positive terminal of the circuit having a potential of 15 V, and the tool is connected to the negative terminal having a potential of -15 V.

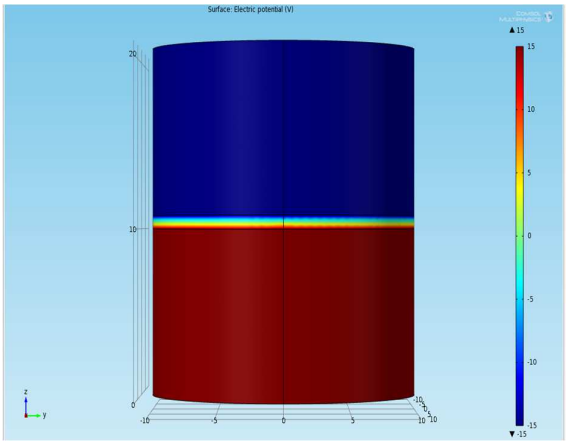

Fig. 8. Electric potential distribution Model 3

Figure 9 shows the electric field distribution for Model 3. The maximum intensity is recorded at the intersection between the anode and cathode. Also, the electric field distribution is uniform along the workpiece.

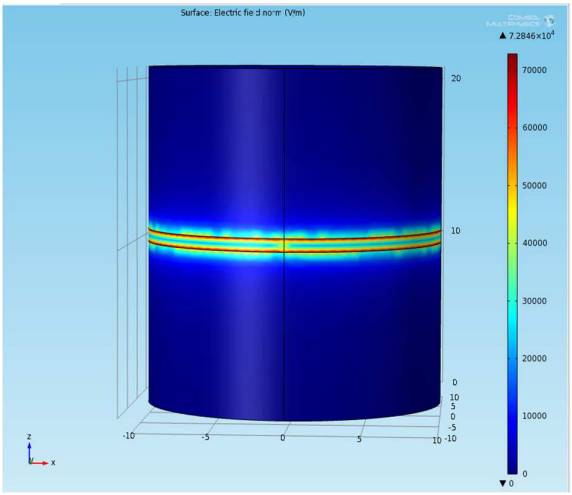

Fig. 9. Electric field distribution Model 3

3. EXPERIMENTAL AND SIMULATION RESULTS

This section presents the simulation results for the associated electric fields. All three electrode pairs are modeled and simulated in COMSOL to determine the maximum electric field, respectively (E_{max}). In the graphs from Figures 10, 11, 12 we can see the electric field distributions for the models.

Based on the simulation results, the location of E_{max} can also be determined, which implies the most likely location of the early processing for the electrochemical machining process.

It is clear that the E_{max} values for all 3 models are recorded at the interface between the workpiece and the electrolyte, respectively between the tool and the electrolyte.

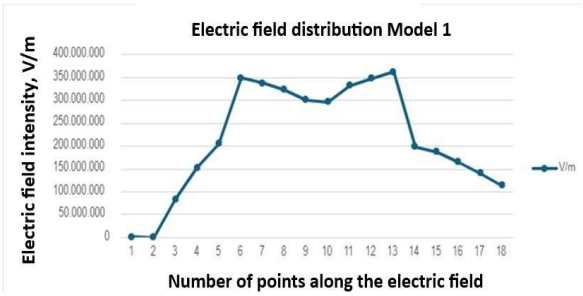

Fig. 10. Electric field distribution Model 1

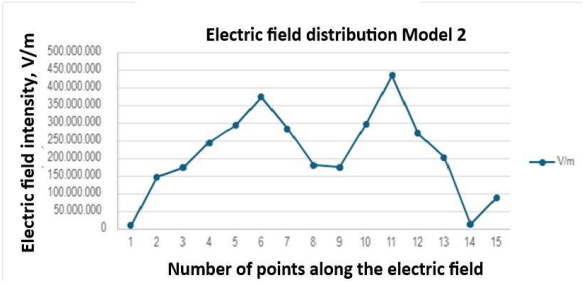

Fig. 11. Electric field distribution Model 2

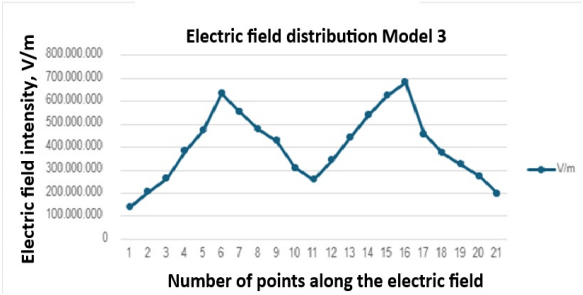

Fig. 12. Electric field distribution Model 3

We can also observe that the highest values among the 3 models are recorded for Model 3, which is due to the higher voltage applied to the model (15 V). Compared to Model 2 (10 V), for Model 3 we observe a 50% increase in E_{max}. As previously mentioned, the only difference between the 2 models is the applied voltage.

Regarding the electrolyte, if we compare Model 1 with Model 2, we observe higher values of the electric field for Model 2 (NaCl 5%). The electric field intensity flux is determined computer-aided using the finite element method, aiming to achieve an optimal size of the components of the electrolytic cell so that, in the area of the surface to be processed, there is a uniformity of the flux.

The finite element model is essential in visualizing the behavior of electric fields under various circumstances, such as the effects of the inter-electrod gap size and the effects of the geometry of the electrodes themselves. In this work, a model for finite element simulation was designed and developed.

4. FURTHER RESEARCH

If the research activity carried out so far has followed the simulation of certain variables such as: electric field and electric potential, in the further research studies I need to:

- design an experimental model;
- create the experimental model;
- test the experimental model;
- optimize the prototype created.

The modeling and simulation of the electrochemical machining allowed me to make an anticipation of the behavior of the system depending on the technological parameters (current, voltage, electrolyte, exposure time), providing a solid basis for the design of the experimental model.

After the design, I will build an experimental model and test it under controlled conditions if the theoretical hypotheses are valid and I will also check the occurrence of unforeseen phenomena in the simulation (e.g. anode wear, deposits, local pH variations).

The validation of the model should highlight both the advantages of the electrochemical machining method (precision, absence of mechanical stress, superior finish) and certain limitations related to electrolyte stability and energy efficiency. The resulting prototype, iteratively improved, should reflect significant advances in process control and surface quality of the machined workpieces. One direction for optimizing the prototype is to optimize electrolyte formulas to reduce environmental impact and increase component durability. Designing a process control for electrochemical machining involves two essential modules. The first involves performing calculations that mimic the ECM process. During the calculations, the chosen process parameters are examined to see if they can reach “critical states”, which would lead to the process being stopped during actual machining. A set of machining parameters that cause a sudden increase in the probability of an electrical short circuit and electrical discharge is known as a “critical state” for an ECM process.

The inter-electrod gap has a significant impact on the analysis of the ECM process. It indirectly determines the degree of oxidation on the anode surface. Also indirectly, changes in one of the calculated physical variables have a rapid impact on the other. This is due to the close relationships between these variables. For example, reducing the inter-electrod gap value leads to a higher intensity of the ECM process. This increases the temperature and conductivity of the electrolytes, which, in turn, leads to greater electrolyte contamination and hydrodynamic resistance. Ultimately, the distribution of the current density or the intensity of the oxidation process of the anode surface are influenced by these factors.

Monitoring the removal of surplus provides a way to drive and control the ECM process. Analysis of the size of the material to be removed is the second control stage that occurs during the machining process. The position of the tool electrode is corrected using comparative analysis to equate the value of inter-electrod gap with the values obtained from the simulation.

At the end of the paper, I will make a comparison of electrochemical processing with conventional methods, in terms of costs and the quality of the resulting workpieces, with a view to possible industrialization.

5. CONCLUSION

The electric field plays a critical role in the entire ECM process; a non-uniform electric field causes material to dissolve more where the field is stronger. The surface of the metal anode material is thought to be continually oxidized and worn away during the electrochemical

machining process, releasing hydrogen gas as the tool cathode's hydrogen atoms get electrons that undergo a reduction reaction. Hydrogen, temperature, and electrolysis products will build up close to the outflow as a result of the electrolyte flowing. Temperature and hydrogen will have an impact on electrical conductivity; therefore, the higher the hydrogen content at the outlet, the lower the current density and electrolyte conductivity.

The geometry of the tool and inter-electrod gap control the final shape of the cavity. The rate of material removal is directly proportional to the electric current density, which depends on the electric field strength. In areas with a strong electric field, dissolution will occur more rapidly, while in areas with a weak electric field, dissolution will be reduced or nonexistent.

At the inter-electrod gap, an electric double layer (EDL) is formed. This affects charge transfer, process efficiency, and the stability of the double layer influences surface accuracy and finish.

Through FEM modeling, the electric field can be optimized:

- to avoid areas of undercutting or overcutting;
- to obtain desired shapes with tight tolerances.
- The electric field is the heart of the ECM process, determining:
- where and how quickly material is removed;
- the shape and quality of the workpiece;
- the energy efficiency and precision of the machining.

Compared to my study, in the studies presented in Chapter 2 the information obtained about the electric field is the following:

1.The pulse ECM evenly distributes the current density.

2.Current density, and side removal rate all progressively rise as the duty cycle increases. The machining accuracy of holes is increased by using a medium duty ratio.

3.A wider lateral gap can speed up the regeneration of electrolytic products and Joule heat while also reducing the range of current density.

4.The hole's width and processing depth increase as the applied voltage rises and the moving tool slows down. This leads to a greater rate of material removal by increasing the current density on the workpiece surface. On the other hand, the machining's aspect ratio is often mild. This is due to the fact that larger inter-electrodes will result from deeper machining, which will slow down the rate of forward corrosion.

5.The distribution of current density is not uniform when the mask is thin (through-mask micro-electrochemical machining). The workpiece center experiences the island-like phenomena, and the aspect ratio is not very good. The mask's shadowing effect is to blame for this. Because the mask is thin, lateral corrosion will be aggressive due to the current density being concentrated on the corners.

6. REFERENCES

[1] Krishna Mohan Agarwal, K., R. K. Tyagi, T., Vikas Choubey, C., Mohd Atif Wahid, W., Arshit Kapoor, K., Ajay Kumar, K., *Enhancements of mechanical properties of materials through ECAP for high temperature applications*, Materials Today: Proceedings, ISSN 2214-7853, vol. 46, part 15, pp. 6490–6495, 2021.

[2] Arjan Minocha, M., *Advanced Manufacturing Techniques in Aerospace Engineering*, Darpan International Research Analysis, ISSN 2582-9474, vol. 12, pp. 50–68, 2024.

[3] Sundar Marimuthu, M., Mohammad Antar, A., Justin Dunleavey, D., *Characteristics of micro-hole formation during fibre laser drilling of aerospace superalloy*, Precision Engineering, ISSN 0141-6359, vol. 55, 2018.

[4] Zhi Li, L., Bin Cao, C., Yu Dai, D., *Research on multi-physics coupling simulation for the pulse electrochemical machining of holes with tube electrodes*, Micromachines, ISSN 2072-666X, vol. 12, 2021.

[5] Xin Zhu, Z., Yadong Liu, L., Jun Zhang, Z., Kai Wang, W., Hong Kong, K., *Ultrasonic-assisted electrochemical drill-grinding of small holes with high-quality*, Journal of Advanced Research, ISSN 2090-1232, vol. 23, pp. 151–161, 2020.

[6] Yuanlong Chen, C., Xiang Li, L., Jinyang Liu, L., Yichi Zhang, Z., *Multiphysics numerical simulation of the transient process in electrochemical machining*, Mechanics, ISSN 1392-1207, vol. 28, pp. 417–422, 2022.

[7] Jie Yao, Y., Y. J. Nie, N., Z. T. Chen, C., *Design and analysis of flow field in electrochemical cutting processing by arranged tube electrode*,

Applied Mechanics & Materials, ISSN 1662-7482, vol. 872, pp. 67–76, 2017.
[8] Ming Chai, C., Zhi Li, L., Hao Yan, Y., et al., *Experimental investigations on aircraft blade cooling holes and CFD fluid analysis in electrochemical machining*, Advances in Materials Science and Engineering, ISSN 1687-8434, 2019.
[9] Weidong Liu, L., Zhen Luo, L., Yang Li, L., Zuming Liu, L., Kangbai Li, L., Jianxiang Xu, X., Sansan Ao, A., *Investigation on parametric effects on groove profile generated on Ti1023 titanium alloy by jet electrochemical machining*, The International Journal of Advanced Manufacturing Technology, ISSN 0268-3768, vol. 100, 2019.
[10] Subrat Patro, P., Dileep Kumar Mishra, M., Julfekar Arab, A., Pradeep Dixit, D., *Numerical and experimental analysis of high-aspect-ratio micro-tool electrode fabrication using controlled electrochemical machining*, Journal of Applied Electrochemistry, ISSN 0021-891X, vol. 50, 2020.
[11] XiaoChao Zhou, Z., ChangYong Cao, C., HongXin Wang, W., Hua Lin, L., *Study on the multi-field coupling model of electrolyte temperature distribution in electrochemical machining*, The International Journal of Advanced Manufacturing Technology, ISSN 0268-3768, vol. 109, pp. 1–8, 2020.
[12] S. Chandrasekhar, C., N. Prasad, P., *Multi-response optimization of electrochemical machining parameters in the micro-drilling of AA6061-TiB_2 in situ composites using the entropy–VIKOR method*, Proceedings of the Institution of Mechanical Engineers, Part B: Journal of Engineering Manufacture, ISSN 0954-4054, vol. 234, no. 10, pp. 1311–1322, 2020.
[13] C.-W. Liu, L., C.-H. Chen, C., S. Lee, L., *Simulation and analysis of through-mask electrochemical machining with moving tools*, Advances in Mechanical Engineering, ISSN 1687-8132, vol. 13, no. 4, 2021.
[14] Xia Hu, H., Dong Zhu, Z., Jun Li, L., Zhen Gu, G., *Flow field research on electrochemical machining with gas film insulation*, Journal of Materials Processing Technology, ISSN 0924-0136, vol. 267, pp. 247–256, 2019.
[15] Albert Nardi, N., Andrés Idiart, I., Paolo Trinchero, T., Luis Manuel de Vries, V., Jorge Molinero, M., *Interface COMSOL–PHREEQC (iCP), an efficient numerical framework for the solution of coupled multiphysics and geochemistry*, Computers & Geosciences, ISSN 0098-3004, vol. 69, pp. 10–21, 2014.
[16] Mohd S. Kamarudin, K., N. H. Radzi, R., A. Ponniran, P., R. Abd-Rahman, A., *Simulation of electric field properties for air breakdown using COMSOL Multiphysics*, Proceedings of the 4th IET Clean Energy and Technology Conference (CEAT 2016), ISBN 978-1-78561-375-9, Kuala Lumpur, Malaysia, 2016.
[17] Rolf Buchner, B., Joachim Barthel, B., Josef Stauber, S., *The dielectric relaxation of water between 0°C and 35°C*, Chemical Physics Letters, ISSN 0009-2614, vol. 306, pp. 57–63, 1999.

Modelarea și simularea diverșilor parametri ai materialelor avansate pentru prelucrarea electrochimică

Rezumat: Această lucrare prezintă multiple simulări numerice ale diverșilor parametri ai materialelor avansate pentru procesul de prelucrare electrochimică (ECM) utilizând software-ul COMSOL Multiphysics. Întrucât nu este posibilă observarea și înregistrarea fizică a proceselor care au loc în interstițiul de lucru, modelarea proceselor este una dintre cele mai eficiente metode de estimare a condițiilor din interstițiul de lucru. În acest context, simularea numerică a procesului electrochimic devine esențială pentru înțelegerea și optimizarea acestuia. Potențialul electric al procesului de prelucrare electrochimică și impactul câmpului electric au fost analizate asupra unei varietăți de materiale avansate pentru a îmbunătăți calitatea procesului ECM.

Titi DANCIU, engineer, PhD student, National University of Science and Technology POLITEHNICA Bucharest, Faculty of Industrial Engineering and Robotics, titi.danciu@stud.fils.upb.ro, +40726806834.
Liviu-Daniel GHICULESCU, university professor, doctor, engineer, National University of Science and Technology POLITEHNICA Bucharest, Faculty of Industrial Engineering and Robotics, daniel.ghiculescu@upb.ro.